ANALYSIS AND TEST CORRELATION OF PROOF OF CONCEPT BOX FOR BLENDED WING BODY-LOW SPEED VEHICLE

Regina L. Spellman
NASA Langley Research Center
1 North Dryden Street
Hampton, VA 23681
757-864-7244
regina.l.spellman@nasa.gov

Abstract - The Low Speed Vehicle (LSV) is a 14.2% scale remotely piloted vehicle of the revolutionary Blended Wing Body concept. The design of the LSV includes an all composite airframe. Due to internal manufacturing capability restrictions, room temperature layups were necessary. An extensive materials testing and manufacturing process development effort was underwent to establish a process that would achieve the high modulus/low weight properties required to meet the design requirements. The analysis process involved a loads development effort that incorporated aero loads to determine internal forces that could be applied to a traditional FEM of the vehicle and to conduct detailed component analyses. A new tool, Hypersizer, was added to the design process to address various composite failure modes and to optimize the skin panel thickness of the upper and lower skins for the vehicle. The analysis required an iterative approach as material properties were continually changing. As a part of the material characterization effort, test articles, including a proof of concept wing box and a full-scale wing, were fabricated. The proof of concept box was fabricated based on very preliminary material studies and tested in bending, torsion, and shear. The box was then tested to failure under shear. The proof of concept box was also analyzed using Nastran and Hypersizer. The results of both analyses were scaled to determine the predicted failure load. The test results were compared to both the Nastran and Hypersizer analytical predictions. The actual failure occurred at 899 lbs. The failure was predicted at 1167 lbs based on the Nastran analysis. The Hypersizer analysis predicted a lower failure load of 960 lbs. The Nastran analysis alone was not sufficient to predict the failure load because it does not identify local composite failure modes. This analysis has traditionally been done using closed form solutions. Although Hypersizer is typically used as an optimizer for the design process, the failure prediction was used to help gain acceptance and confidence in this new tool. The correlated models and process were to be used to analyze the full BWB-LSV airframe design. The analysis and correlation with test results of the proof of concept box is presented here, including the comparison of the Nastran and Hypersizer results.

Introduction

The Blended Wing Body (BWB) is a radical new aircraft design based on the flying wing concept. The BWB has been studied by NASA and Boeing for a large commercial or military aircraft for passenger and/or airfreight transportation. It is believed the BWB would consume 20% less fuel than traditional jetliners flown today. NASA LaRC has been working on a BWB - Low Speed Vehicle (BWB-LSV) that is a 14.2% scale model of the BWB. The primary goals of the BWB-LSV project are to study the flight and handling characteristics of the BWB design, compare the actual vehicle's performance with predictions from computer and wind tunnel studies, develop and evaluate digital flight control algorithms, and to assess the integration of the propulsion system to the airframe.

The LSV is a 2500 lb, 35-foot wingspan, remotely piloted research aircraft. It contains all the complexity of an actual airplane including three engines, landing gears, fuel system, flight termination system, and a spin chute recovery system. The solid model of the LSV is shown in Figure 1.

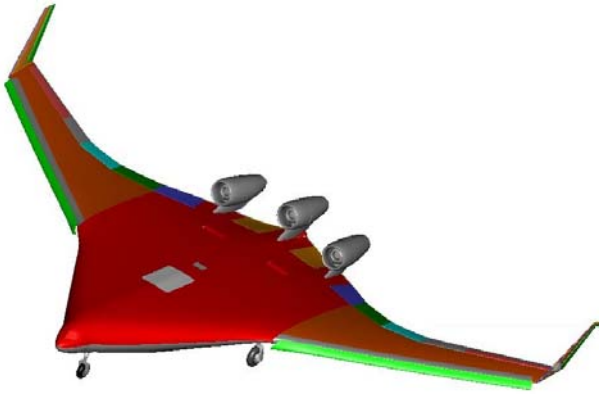

Figure 1: BWB-LSV

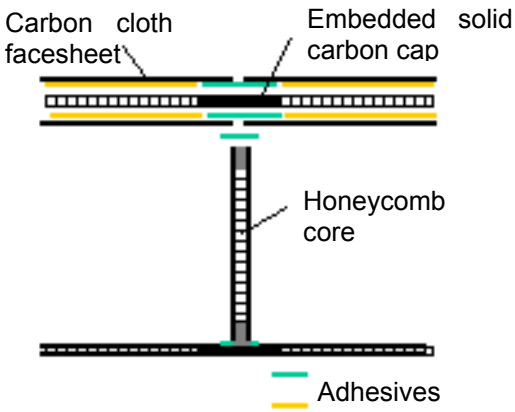

Figure 2: Rib and Skin Cross Section

The dynamic scaling requirement for the LSV caused great difficulty for designing an airframe that has the necessary strength and stiffness within the strict weight limits. Due to the unusually large size of the vehicle, there were limitations to LaRC's in-house composite fabrication capabilities and resources. These combined restrictions limited the design to a room temperature cure composite design. An extensive materials characterization effort was implemented to identify materials and processes that could be used to meet the demanding requirements.

The airframe is designed from small composite panels that are fabricated separately and assembled in a building block technique. The webs are bonded to the skins and at spar and rib intersections. Aluminum fittings (x-clips) are also used to join the webs together at rib and spar intersections. These x-clips are used for alignment as well as load transfer. The panels consist of a honeycomb core with carbon cloth facesheets. The number of plies of cloth is customized for each bay area to minimize the weight of the vehicle. A solid carbon cap is incorporated for the ribs and spars. This cap is the main load-carrying member. The caps are embedded in the honeycomb skin panels. A schematic of a typical cross section is shown in Figure 2. In this figure, the honeycomb and carbon cloth facesheet construction is shown along with the embedded solid carbon caps.

A Proof of Concept box (POC box) was initiated early in the material characterization to test this fabrication process. The box was fabricated from the materials that had been identified at that phase of the design development. After the fabrication techniques had been verified, the box was available for load testing. The proof of concept box was representative of a simple wing box, consisting of skins, ribs, and spars. For testing, the box was cantilevered off a backstop and loaded in shear, torsion, and bending. The box was then tested to failure in shear. This would contribute to the validation of the fabrication processes. The test results were also used to study the analytical techniques being developed for the full vehicle analysis process. A full-scale proof wing would be fabricated and tested further in the project cycle. The proof box (the top skin not yet attached) is shown in Figure 3.

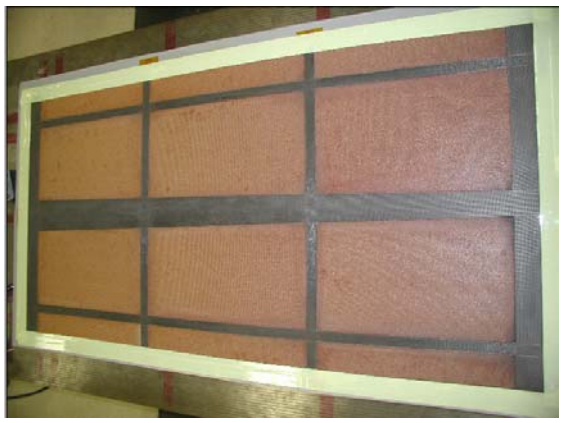

Figure 3: POC Box

This report discusses the analysis of the POC box and the results of the tests. The correlation between analysis and test is discussed along with recommendations for future analyses in support of the BWB-LSV project.

The POC box was analyzed using the same methods that would be implemented in the full vehicle analysis. A finite element analysis (FEA) was first completed of the box and this was used as the model and load definition for the Hypersizer analysis. The process is

described in more detail in the following sections.

POC Box Description

The completed box was 60"Lx30"Wx3"D and weighed 13.2 lbs. It consists of upper and lower honeycomb skins, three spars, and two ribs. Each of the spars and ribs is bonded to the caps, which are embedded in the skins. All spar and rib caps are 1" wide except for the center spar cap. This cap is tapered from 4" wide at the fixed end to 2" wide at the loading end. Aluminum x-clips are present at each spar/rib intersection. Aluminum end fittings were also incorporated at each end of the box for load application and mounting.

The top and bottom skins were constructed of a 0.125" thick honeycomb core (Hexcel HRH-10-1/8-1.8) with a single ply of +45/-45 3.5 oz carbon cloth facesheet. Each ply is 0.006" thick. The shear webs were 0.25" thick honeycomb, also with a single ply of the same carbon cloth facesheet. The spar caps were 1/8" thick layups of 0/90 5.8 oz carbon tape. The carbon cloth and tape properties are included in Table 1. The honeycomb properties are provided in Table 2.

Table 1: Composite Properties

Property	**Graphite 3.5 oz. cloth 24/24 weave**	**Graphite 5.8 oz. cloth 12/12 weave**
ρ (lb/in.^{3})	.052	.052
E_t (Msi)	2.28	9.13
G (Msi)	1.14	0.637
ν	.822	.056
$\sigma_{t,\,ult}$ (ksi)	20	101
$\sigma_{c,\,ult}$ (ksi)		68
$\tau_{,ult}$ (ksi)	16	13

Table 2: Honeycomb Properties

		Strength (psi)	Modulus (ksi)
Compressive (Stabilized)		95	8
Plate Shear	L Direction	75	3.8
	W Direction	40	1.5

Analysis Description

One of the objectives of the analysis was to validate analytical techniques being developed for the full vehicle analysis. For this reason, the models were generated as similar to the existing global vehicle models as possible. The same analytical tools were used. All FEM variables were kept consistent for these models wherever possible. However, the analysis was also used to refine this process. In some instances, suggested improvements to the modeling technique were identified. These are noted in this document where appropriate.

The POC box FEA was completed using MSC/Nastran [1]. MSC/Patran was used for the pre- and post-processing. The model was generated using CQUAD4 elements (with PCOMP property sets) for the skins, ribs, and spars. CBEAM elements were used to model all spar and rib caps, except for the center spar cap because of the thickness and taper. Sensitivity studies showed modeling this wider cap with CQUAD4 elements improved the accuracy of the FEM. HEX8 elements were used to model the aluminum end fittings. Similar to the full vehicle Loads FEM generated by Boeing, the aluminum x-clips at the spar-rib intersections were not included. The intersections were assumed continuous. The POC box FEM is shown in Figure 4. In this figure, the fixed end boundary condition and the torsion loading are shown. Figure 5 shows the different property sets of the shell elements. The tapered spar cap can be seen in the upper skins. The solid aluminum end fittings are not shown in this figure.

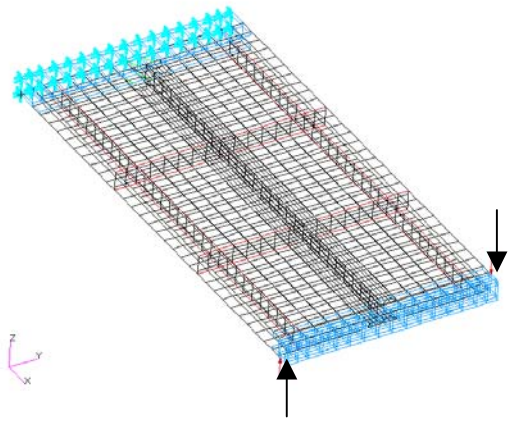

Figure 4: Finite Element Model

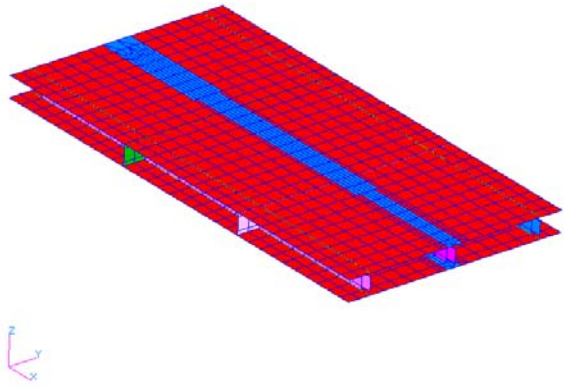

Figure 5: Property Sets

The POC box was modeled as cantilevered from the root end. Because a solid aluminum end fitting was used, each node on the face of the fitting was constrained in all six DOFs. The load was applied to the solid elements at the opposite end. Three load cases were considered. These include a 1000 in-lb bending moment, 1000 in-lb torsion, and 70 lb shear. The moments were applied as forces with the appropriate moment arm.

To address the assumption of true fixedness in the end of the proof box, a calibration box was examined. The idea behind this calibration box was to analyze and test a box of well-known properties. The correlation between the test and analysis would indicate if the cantilever was truly fixed, or if it had some extent of reduced stiffness. This reduced stiffness could be applied to the POC box. The calibration box was fabricated from aluminum. It was mounted and loaded in an identical manner as the proof of concept box. The calibration box results indicated that the method of constraining the box was adequate and no reduced stiffness boundary condition was needed.

The next phase of the analysis process was to analyze the local composite failure modes. Instead of the traditional closed form calculation method, the commercial code Hypersizer was identified for this task. Hypersizer is a composite panel analysis code that is typically used as an optimizer in the design process [2]. Hypersizer can quickly analyze multiple design concepts under a variety of load cases and identify the optimal design based on a variety of parameters. For the full vehicle, it will be used to do the actual sizing of each skin panel for the hundreds of load cases necessary. However, for the POC box, the design and material properties were already established. The POC box had been fabricated from minimum gauge thicknesses because it was initially only thought to be a fabrication exercise and not a complete test article. With the intent of validating the analytical process, Hypersizer was included in this effort as it would be for the vehicle. The MSC/Nastran model was imported into a Hypersizer database and analyzed for the one design configuration. In this particular case, the results could be used to back out a predicted failure load for the given design.

Hypersizer analyzes the box as panels as opposed to the small regions in a finite element model. A “high stress area” is not defined as in traditional finite element codes. Rather, this code identifies a wide variety of composite failure modes that are not predicted in an FEA. The individual elements from the FEM are consolidated into components, such as center spar, top skin, bottom skin, etc. Elements with the same Nastran property set are defined as a single component in Hypersizer and analyzed as a single panel. Although the skins/spars have the same properties, they were defined as unique property sets in the Nastran model to create smaller components in Hypersizer. In particular, near the root of the box, the skins were broken up into separate sections between each rib and spar. This was done in order to isolate the failure location. Instead of determining the load for the entire upper skin, the failure mode could be isolated by section. The different components are shown in Figure 6. The loads from the finite element model are used to determine edge loadings for each component. These edge loads are used in the failure analyses. A minimum margin of safety is then identified for all failure methods examined. For this analysis, all factors of safety were defined as 1.0. The load was then scaled to achieve a minimum Margin of Safety (MOS) of 0.0. With an MOS equal to 0.0, the applied load is equivalent to the allowable load. Therefore, the ultimate failure was predicted to occur at the load resulting in a zero MOS. It should be pointed out that not all failure mechanisms would result in catastrophic failure. This was considered in the analysis. The load was scaled to match the first significant failure mode. For secondary failures, the MOS was allowed to reach negative numbers (indicating that particular failure had already occurred).

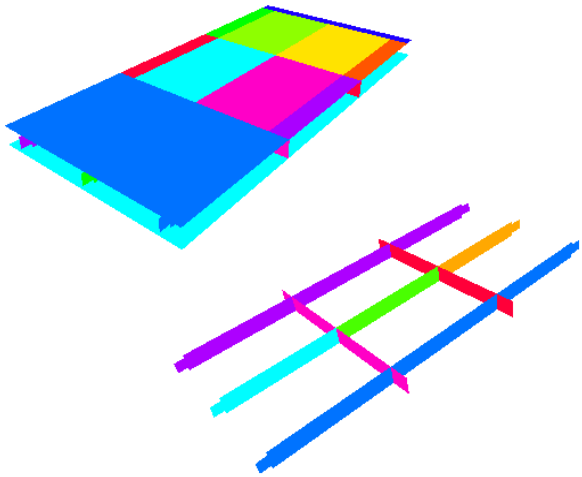

Figure 6: Hypersizer Components

Table 4: FEA Von Mises Results

Load Case	Location	$\sigma_{vm,max}$ (ksi)
70 lb Shear	Skins	1.19
	Ribs/spars	1.20
	Center spar cap	2.00
	All other caps	2.44 (axial)
1000 in-lb Bending	Skins	0.47
	Ribs/spars	0.60
	Center spar cap	0.75
	All other caps	0.61 (axial)
1000 in-lb Torsion	Skins	0.71
	Ribs/spars	0.42
	Center spar cap	1.17
	All other caps	2.03 (bending)

Analytical Results

The analytical prediction of deflection and Von Mises stress for the three different test conditions are outlined in Table 3 and Table 4, respectively. The maximum stress is identified for each major property set. Assuming a linear solution, the results for the shear load case can be scaled to predict the ultimate load. The caps are made from a very high strength material, leaving the lowest MOS in the skins or ribs and spars. Using the maximum stress of 1.2 ksi in the spars and assuming a 20 ksi ultimate strength (σ_{all}) for the skins, a linear extrapolation results in a predicted failure shear load of 1167 lbs. However, the actual failure occurred in the proof box at 899 lbs. At this loading, the Nastran model still predicts positive MOS as shown in Table 5. Von Mises Stress plots are shown for the shear, bending, and torsion load cases in Figure 7, Figure 8, and Figure 9, respectively.

Table 5: MOS for Ultimate Load (899 lbs)

	$\sigma_{vm,max}$(ksi)	σ_{all} (ksi)	MOS
Skins	15.4	20	0.23
Ribs/spars	15.4	20	0.23
Center spar cap	25.7	68	0.62
All other caps	31.3 (axial)	68	0.54

Table 3: FEA Displacement Results

Load Case	Max Deflection, inches
Shear	0.17
Bending	0.156
Torsion	0.004
Ultimate (899 lbs)	2.19

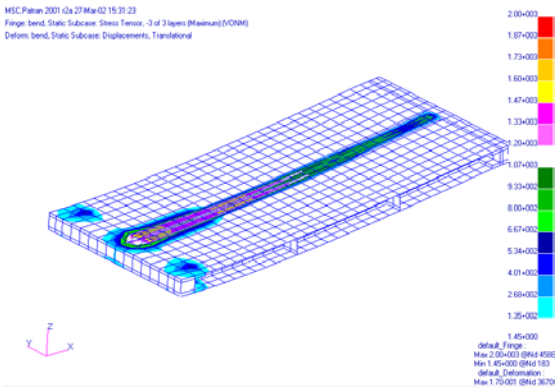

Figure 7: Shear Load Case – Von Mises Stress Plot

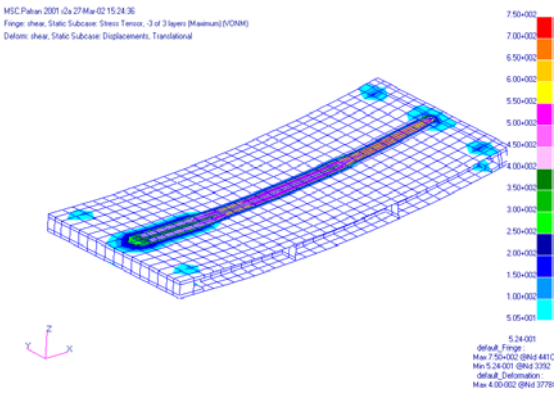

Figure 8: Bending Load Case – Von Mises Stress Plot

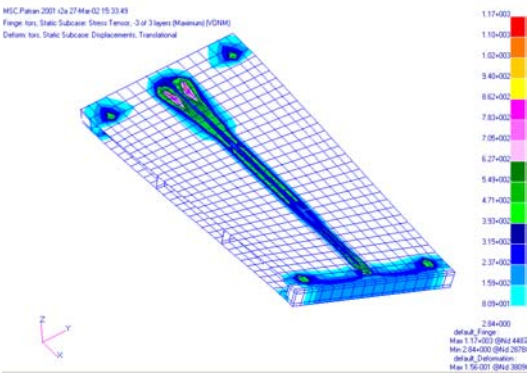

Figure 9: Torsion Load Case - Von Mises Stress Plot

The results of the FEA were imported into Hypersizer. The shear, bending and torsion cases were all examined. Each showed significant positive MOS. For this analysis, a load factor of 1.0 and the zero-sigma averaging was used. A shear load of 899 lbs was then analyzed to compare the Hypersizer prediction to the actual failure. The predicted failure mechanism was composite strength of the sandwich face. The MOS at 899 lbs for each major component is listed in Table 6. This resulted in the minimum MOS of 0.06 occurring in the center spar. Similar to the Nastran results, the shear load results were scaled linearly to predict the approximate ultimate failure load (MOS=0.0). Based on these results, a failure load of 960 lbs was predicted.

Table 6: Margin of Safety for Major Components at Ultimate Load 899 lb

Component	MOS	Mode
Skin	.25	Intracell dimpling
	.6	Panel buckling
Center Spar	0.06	Composite strength
Right/Left Spar	0.56	Composite strength
Ribs	.36	Intracell dimpling
	2.6	Composite strength
Center spar cap	.19	Buckling

Experimental Set Up

The proof of concept box and the aluminum calibration box were tested in an identical fashion. The boxes were both mounted to a backstop as shown in Figure 10. The POC box is shown in this figure. To apply the bending moment and torsion, a set of pulleys was used to transfer a vertical load into a moment. The pulleys used for the torsion test can be seen at the free end of the POC box in Figure 10. A special “T” fixture was fabricated to apply the bending moment. The fixture was attached to the free end of the box. The pulleys were on the extended leg of the “T” fixture. For the shear loading, a hydraulic jack was used to apply the loading to the center of the free end. This can also be seen in Figure 10.

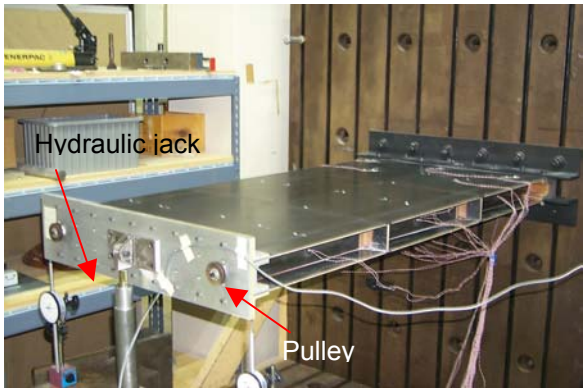

Figure 10: Test Set-up

On the POC box, 26 strain gage stations were instrumented (most with rosette strain gages) for a total of 62 channels of strain data. These included the upper and lower skins and shear webs. Figure 11 shows the internal strain gage locations and Figure 12 shows the external locations. Twelve single axis accelerometers

were placed on the centerline of the upper surface to measure the displacements along the length of the box. A Leica tracking system was also used to measure deflection. The data points and Leica target can be seen in Figure 13. For the final ultimate load test, the method to measure displacements had to be modified to prevent damage to the system. To solve this problem, two dial indicators were placed at the left and right front corners to measure tip deflection (Figure 14). These indicators were read manually as the test progressed. Also for the final load test, a film of talcum powder was applied to the upper surface. The powder was used to provide visual detection of any possible deformation or delamination.

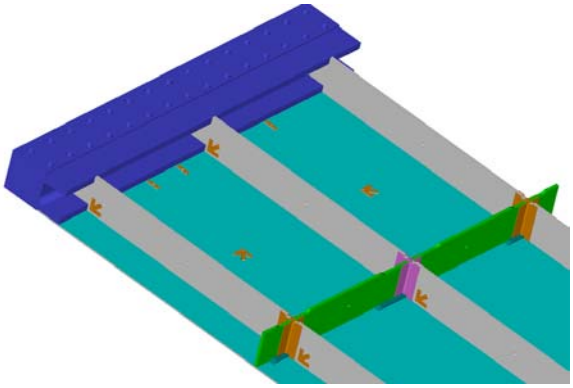

Figure 11: Strain Gage Locations, Internal

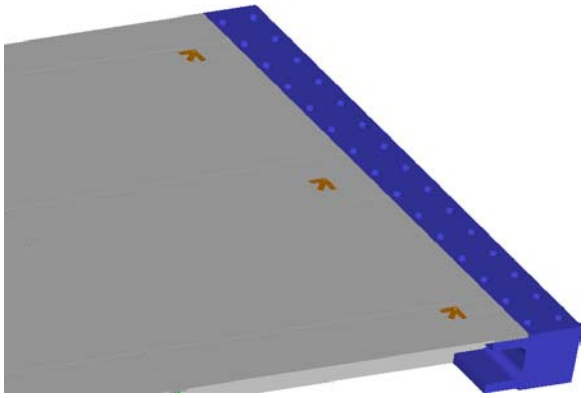

Figure 12: Strain Gage Locations, External

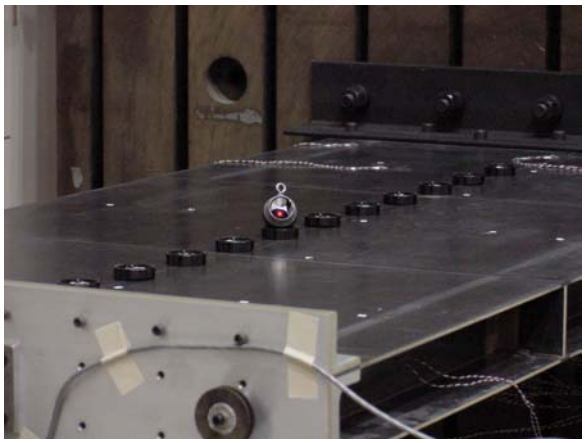

Figure 13: Leica Tracking System

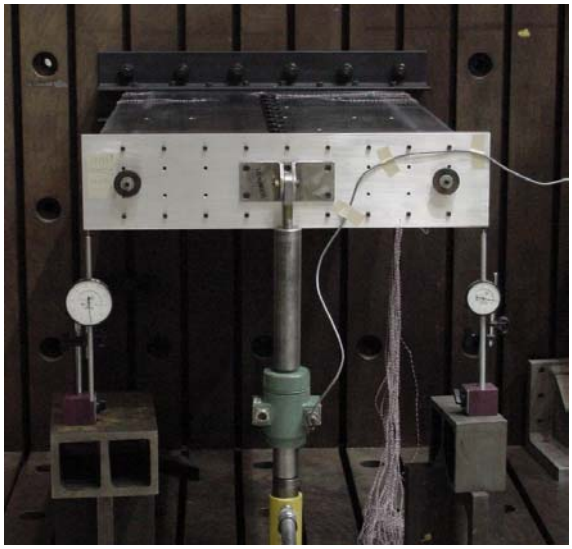

Figure 14: Dial Indicators for Ultimate Load Test

Tests included a shear, torsion, bending, and ultimate load. The torsion test was used to determine an equivalent shear modulus of the assembly, based on $\theta=(TL)/(JG)$. The bending test was used to determine an equivalent modulus of elasticity based on $\Delta=(ML)/(EI)$. The ultimate test would identify the failure mode and location, for comparison to the Hypersizer analysis. A modal test was conducted prior to all testing and in between each test to insure the health of the box. A final modal test was conducted after failure [3].

Experimental Results

Figure 15 shows deflection along the centerline down the length of the box for 1000 in-lb bending moment and Figure 16 shows the deflection down the length of the box on either edge for 1000 in-lb torsion. These figures also include a comparison with the analytical

prediction, obtained from the Nastran model. In both figures, the experimental data are shown as the discrete points. The FEA results are the smooth continuous curves. In Figure 15, the analytical and experimental results show good comparison, however the slopes of the curves are different. The experimental results indicate the box is slightly stiffer than modeled at the root, but less stiff than modeled at the free end. In Figure 16, the FEA results are symmetric as would be expected for an applied torsion loading. However, the experimental results are slightly nonsymmetrical. It is unknown if this error is due to a nonsymmetrical load application or errors in the measurement system.

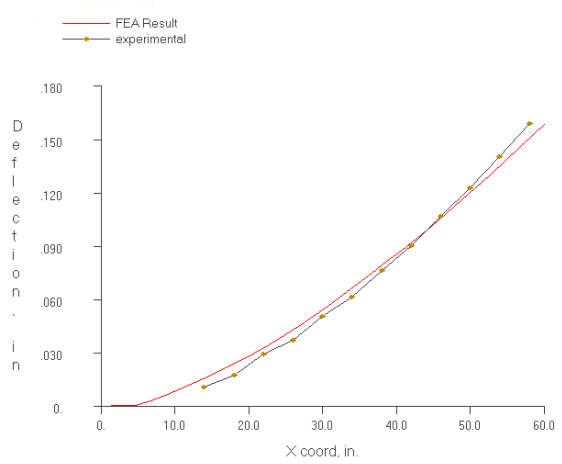

Figure 15: Deflection along centerline for bending moment = 1000 in-lb

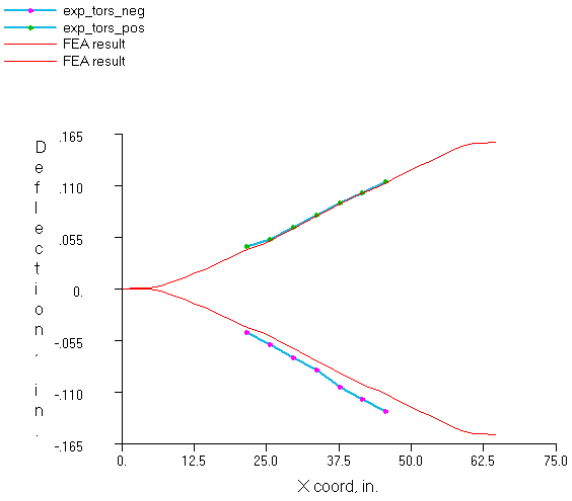

Figure 16: Deflection along edges for 1000 in-lb torsion

The strain gage data for the first three tests (bending, shear, and torsion) were analyzed. Due to such low loading levels and possible problems with the data acquisition system, the data were of little use. An improved system was utilized for the final test. A typical strain plot is shown in Figure 17. The data is from the upper and lower skins near the root (gages shown in Figure 12). In this figure, six gages are shown. The vertical dashed lines represent the loads at which the "pops" were heard. This is reflected in the strain data for the lower skins where steps can be seen, indicating possible delaminations.

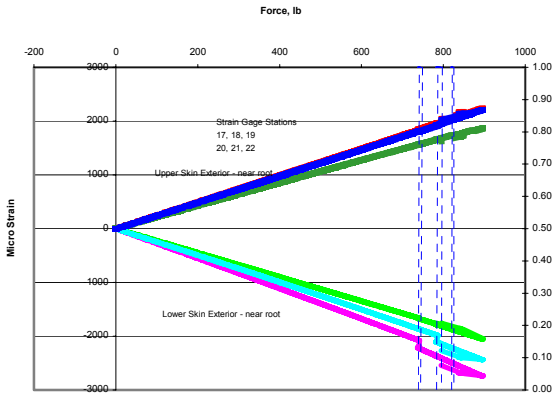

Figure 17: Strain Gage Data

Ultimate Load Test

The final test to be completed was the ultimate load test. The POC box was loaded until failure occurred. Figure 18 below shows the load versus deflection. Final failure and earlier "pops" observed are noted on this curve. The final catastrophic failure occurred at 899 lbs. Investigations following the test concluded the failure occurred in the center shear web. The observed "pops" appeared to be a result of skins delaminating that did not result in catastrophic failure.

Following the test the POC box was dissected for closer examination. From this examination, it was apparent the center main spar web had failed. Figure 19 shows the failure. A crack can be seen that propagates from the top to the bottom at a 45° angle. In Figure 20, the box is viewed upside down. An additional crack can be seen running along the bottom edge of the web (upper in photo).

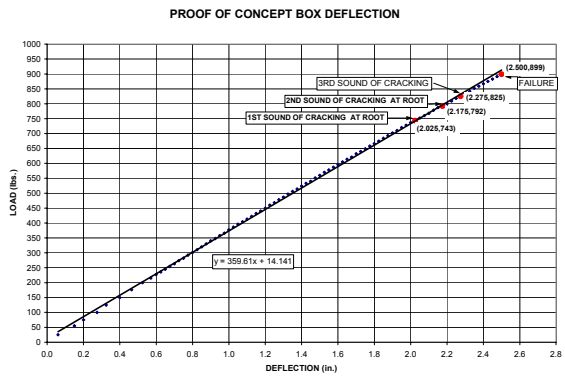

Figure 18: Load vs. Deflection in Ultimate Load Test

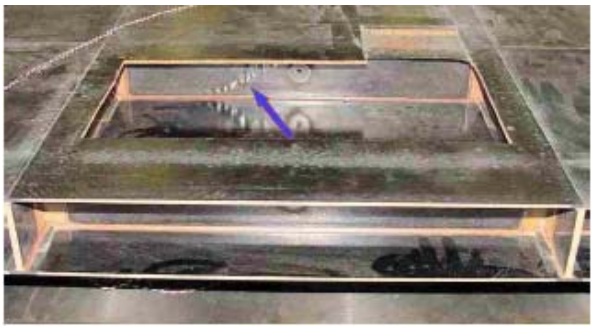

Figure 19: POC Box Failure

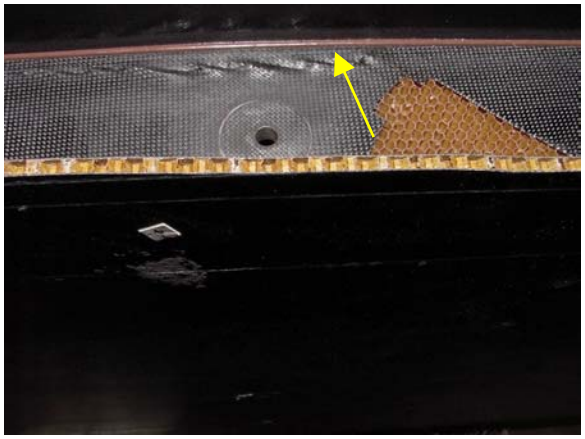

Figure 20: Failed Shear Web (viewed upside down)

Modal Study

A modal study was conducted on the POC box that included the FEA and a modal survey [3]. The FEA results indicated a first and second bending frequency of 12.6 Hz and 104 Hz, and a first torsion frequency of 22 Hz. The modal survey identified the first and second bending frequencies at 12.9 Hz and 110 Hz. However, the first torsion mode was identified at 38 Hz. The results were not available to conduct a modal correlation and model update.

The modal survey was used as an in-situ method of detecting failure between tests. A "frequency fingerprint" was obtained before any testing was conducted, and following each of the three load tests to verify that no discontinuities had developed prior to the ultimate load test. The final modal survey did not show significant changes in the modes below 110 Hz. However, a significant difference was observed in the higher modes. This was the expected outcome once the failure mode was identified. A failed center web should not greatly affect the bending modes. For the proof wing and full vehicle tests, the modal survey should be conducted in a more detailed fashion. Rather than trying to excite only the primary modes, each bay should be impacted. By impacting each bay, local delaminations could be better identified. The limited survey on the box would not be as effective on a larger scale item.

Conclusions

Typically, Nastran or other finite element analysis tools are used as the sole method for verifying design. As is evident from this study, the FEA alone was not sufficient due to the composite failure mechanisms. Hypersizer was used to quickly analyze for the local composite failure modes. Utilizing the model, property sets, and loads from the Nastran analysis made this additional analytical step relatively inexpensive in terms of schedule and resources.

Table 7 summarizes the different predicted ultimate failure loads compared to the actual. Combined, the FEA and Hypersizer were very effective in predicting the composite failure. Based on these results, it is believed that this process can be used with confidence in analyzing the full LSV vehicle. In addition, it is believed that incorporating both tools leads to a more reliable analysis.

Table 7: Predicted vs. Actual Ultimate Load

Method	Load	% Error
Nastran	1167	29.8%
Hypersizer	960	6.7%
Actual	899	--

It should be noted that the results indicate a high accuracy in the Hypersizer analysis in predicting the ultimate load. However, this is not the conclusion from this analysis. The material properties used were themselves results from limited coupon testing. The load testing techniques were not the most accurate available. Combined, these introduce significant

unknowns in the analytical and experimental results. However, it is believed that the FEA and Hypersizer combination is a much more effective method than traditional analyses alone, and should be used for verifying composite designs.

References

[1] MSN/Nastran Quick Reference Guide Version 70.5, The Macneal-Schwendler Corp., 1998

[2] Collier, C., Yarrington, P., Pickenheim M., The HyperSizing Method for Structures, Proceeding of NAFEMS World Congress '99, April, 1999

[3] Werlink, R. J., Composite Bending Box Section Modal Vibration Fault Detection, NASA Langley Report, 2002